Reprinted from Preprint Volume: 21st Conference on Radar Meteorology, September 19-23, 1983, Edmonton, Alta., Canada. Published by the American Meteorological Society, Boston, Mass.

17.7

MICROBURSTS IN JAWS DEPICTED BY DOPPLER RADARS, PAM, AND AERIAL PHOTOGRAPHS

T. Theodore Fujita
The University of Chicago
Chicago, Illinois

Roger M. Wakimoto
UCLA
Los Angeles, California

1. INTRODUCTION

In the early 1970's, photographs taken during aerial surveys performed by the University of Chicago revealed divergent patterns of high-wind damage in cornfields and forests after severe storm activity. These pictures suggested that some downdrafts, under certain conditions, could produce tornado-like damage at the surface. Of particular interest was a class of these violent outflows called "microbursts" which occur on a spatial and temporal scale of 1 to 4 km and 2 to 5 min, respectively, and have been a causal factor in a number of aircraft accidents (Fujita & Byers, 1977; Fujita & Caracena, 1977; NTSB, 1983).

As a result of these recent findings, the NIMROD (Northern Illinois Meteorological Research On Downbursts) Project was operated near Chicago, Illinois in the spring and summer of 1978 to gain an understanding of this phenomenon (Fujita, 1979; Fujita & Wakimoto, 1982). Unfortunately, the NIMROD network was too coarse to obtain detail multi-Doppler information, although excellent single-Doppler data were collected on several microburst events (Fujita, 1980). Based on the knowledge obtained from the NIMROD data set, it was clear that if another project was established, it would have to include a small triple-Doppler triangle and the surface PAM stations would have to be densely distributed in order to depict the three-dimensional structure of the microburst in space and time. The joint effort of the University of Chicago and the National Center for Atmospheric Research (NCAR) resulted in the operation of the JAWS (Joint Airport Weather Studies) Project near Denver, Colorado in the spring and summer of 1982 (McCarthy, Wilson, & Fujita, 1982).

The purpose of this paper is to present preliminary results obtained from the JAWS Project using Doppler radar, PAM, and aerial photography. Section 2 discusses the definitions of the microburst phenomenon. Statistics comparing NIMROD (Midwest region) with JAWS (High Plains region) microbursts are presented in Section 3. Section 4 discusses the possible parent clouds of the microburst, and an analysis of a macroburst/microburst event on 14 July 1982 is presented in Section 5.

2. DEFINITIONS OF DOWNBURSTS AND MICROBURSTS

After the investigation of the Eastern 66 accident at New York City's JFK Airport on 24 June 1975, Fujita, proposed the term "downburst" to describe the outflow which affected the airport.

Downburst: a strong downdraft which induces an outburst of damaging winds on or near the ground.

By 1978, it became apparent that there were two types of downbursts which occurred on different temporal and spatial scales, as a result the term was sub-divided into "macroburst" and "microburst".

Microburst: small downbursts, less than 4 km in outflow size, with peak winds lasting only 2 to 5 min. Microbursts induce dangerous tailwind and downflow wind shear which can reduce aircraft performance.

Macroburst: large downbursts with 4 km or larger outflow size with their damaging winds lasting 5 to 20 min. Intense macrobursts cause tornado-like damage up to F3 in intensity (Fujita & Wakimoto, 1981).

Understanding the mechanism of the microburst was one of the primary objectives of the JAWS Project. Its effect on aircraft performance was tragically illustrated by the crash of Pan American Flight 759 at New Orleans on 9 July 1982. The NTSB report (NTSB, 1983) confirmed that 1) the accident aircraft encountered microburst-induced wind shear and 2) the limited capability of current ground-based low-level wind shear detection technology also contributed to the accident. An analysis of the microburst at the time of the accident is shown in Fig. 1. Examples of the relationship between microbursts and much larger scale gust front (Charba, 1974; Goff, 1976; Wakimoto, 1982) are shown in Figs. 2 and 3.

During the field phase of JAWS it was concluded that some microburst winds occur in heavy rain while others are associated with virga shafts with no measurable precipitation at the surface. Based on the amount or precipitation measured during a microburst, the term was divided into "dry" and "wet" microburst.

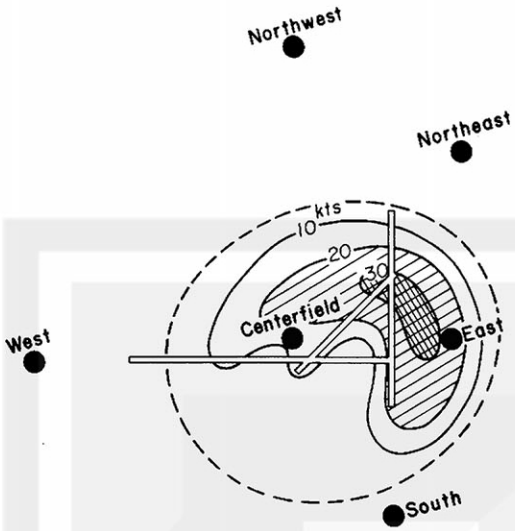

Fig. 1. Wind field of the microburst at the time of the Pan American accident at New Orleans on 9 July 1982. The black dots denote the location of the LLWSAS (Low-Level Wind Shear Alert System). Note that only two stations were affected by the microburst winds.

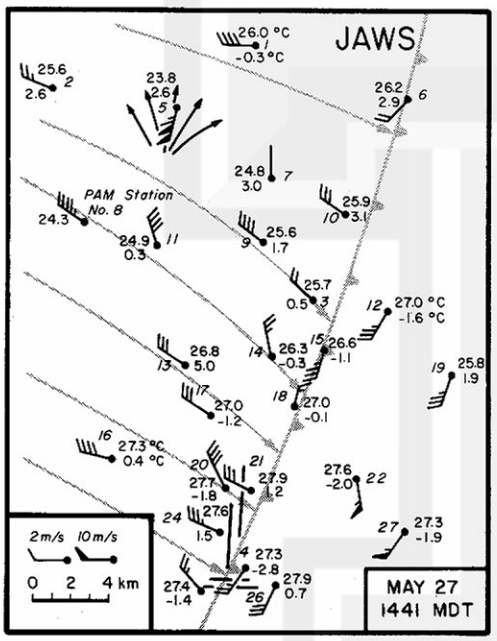

Fig. 2. Example of a microburst at station No. 5 on 27 May 1982 behind the gust front. The gray lines denote the overall gust front winds.

Dry Microburst: a microburst that is accompanied by less than 0.01" of rain between the onset and the end of the high winds, including calm periods if any.

Wet Microburst: a microburst that is accompanied by 0.01 or greater inches of rain between the onset and the end of the high winds, including calm periods if any.

Several observations during NIMROD and JAWS confirmed the need to classify a microburst based on the height of the maximum winds, resulting in the term "surface" and "midair" microburst.

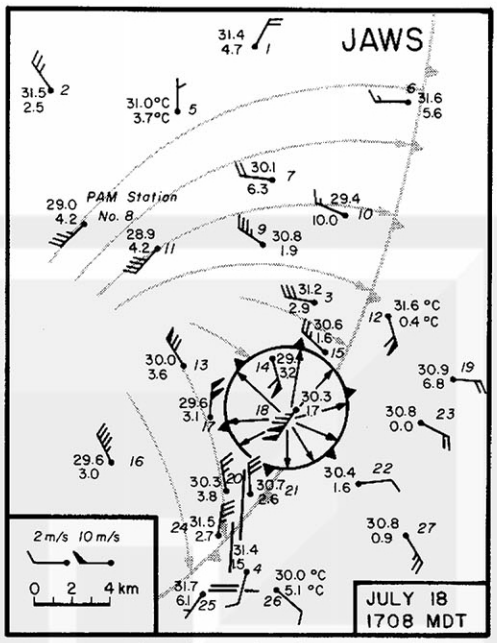

Fig. 3. Example of a microburst on 18 July 1982 on a gust front. The gray lines denote the overall gust front winds.

Surface Microburst: a microburst with its outburst winds detectable by a dense network of ground-based anemometers. The maximum wind speeds are often located less than 100 m (300 ft) above the ground.

Midair Microburst: a microburst aloft with its outburst wind located above the detectable height of ground-based anemometers. Within several minutes the outburst winds may descend to the ground becoming a surface microburst or it may remain aloft and dissipate.

A schematic model of the midair and surface microburst is shown in Fig. 4. Note that a midair microburst that does not reach the surface can still induce an unexpected wind shear that affects aircraft performance.

3. MICROBURST STATISTICS - A COMPARISON BETWEEN NIMROD AND JAWS

In an attempt to ascertain the characteristics of surface microbursts during NIMROD and JAWS, all of the PAM data for both networks were analysed by computer. The 27 surface stations were in the field for 43 and 86 days during NIMROD and JAWS, respectively, collecting data for ∿95-97% of the total operational period. An objective technique was applied to every one-minute of wind data resulting in 436 suspected microbursts in JAWS and 143 in NIMROD. For each of these cases, 15-min wind data centered at the peak microburst wind speed were plotted on a synoptic map along with time sections of wind speed, wind direction, temperature, dew-point temperature, and station pressure. The final selection was made by analysing the synoptic maps and time sections, reducing the total number of microbursts to 186 for JAWS and 50 for NIMROD. These two data sets should be representative of microburst activity over the Midwest (NIMROD) and over the High Plains (JAWS).

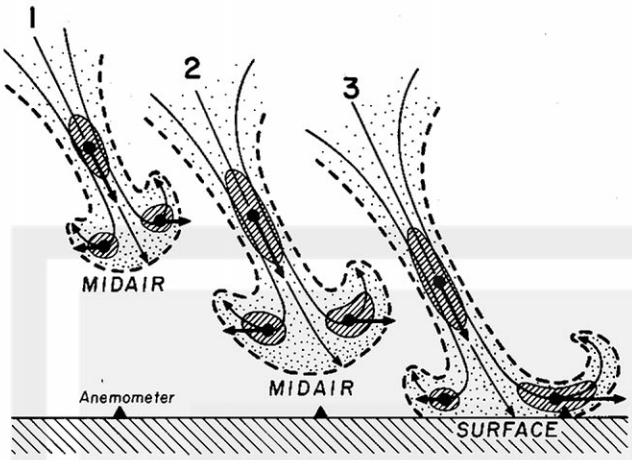

Fig. 4. Transient features of a descending microburst. Hatched areas represent pockets of high winds. Some midair microbursts descend to the surface becoming surface microbursts while others remain aloft. Midair microbursts cannot be detected by ground-based anemometers until they reach the surface.

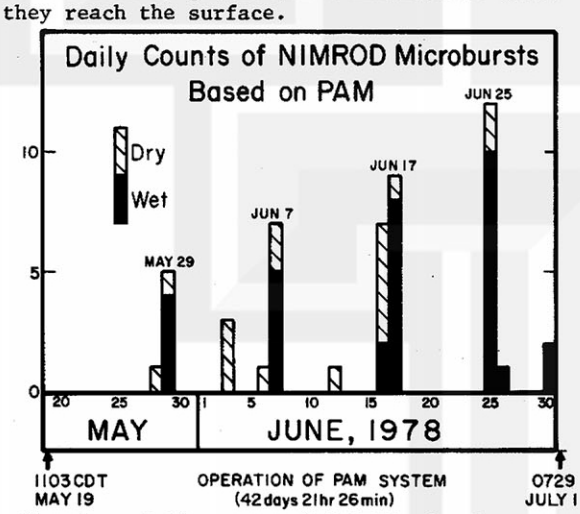

Fig. 5. Daily count of NIMROD microbursts as determined by computer analysis. The number of wet and dry microbursts is shown on the figure.

3.1 Daily Count of Microbursts

The daily count of NIMROD microbursts is shown in Fig. 5. Interestingly, the microbursts occurred predominantly on several convectively unstable days, approximately nine days apart. Of the 50 microbursts in NIMROD, 18 were dry and 32 were wet.

During the 83 days of the JAWS Project there were 49 microburst days as illustrated in Fig. 6. The total of 186 microbursts was sub-divided into 31 wet and 151 dry microbursts which suggests, as expected, that dry microbursts are more frequent over the High Plains than over the Midwest. Unlike NIMROD, where microburst activity appears to be related to synoptic scale forcing, activity during JAWS is strongly influenced by local effects, with solar heating being the most important factor.

3.2 Diurnal Variation of Microbursts

Fig. 7 shows the diurnal variation of microbursts for JAWS and NIMROD. The effect of solar heating during JAWS is clearly evident as microbursts rarely occur before 1100 MDT or after 2300 MDT. Both dry and wet microbursts increase rapidly around noon reaching a significant peak at ~1800 MDT. The second peak frequency of wet microbursts is reached later in the day, between 1900 and 2000 MDT.

Most microbursts during NIMROD occur between 1500 MDT to midnight with insignificant peaks extending from 1000 MDT to midnight. The occurrance of microbursts late into the night is not surprising considering the high number of nocturnal thunderstorms over the Midwest in the summer.

3.3 Rainfall Rates versus Microburst Wind Speeds

There does not appear to be a relationship between rainfall rate and the maximum outburst winds during NIMROD (Fig. 8). The strongest microburst wind, 31.3 m/s was accompanied by a rainfall rate of 1.1 inches per hour. This suggests that an ominous-looking shower may not produce damaging winds, and that precipitation drag is not the main factor in determining downdraft speeds in microbursts.

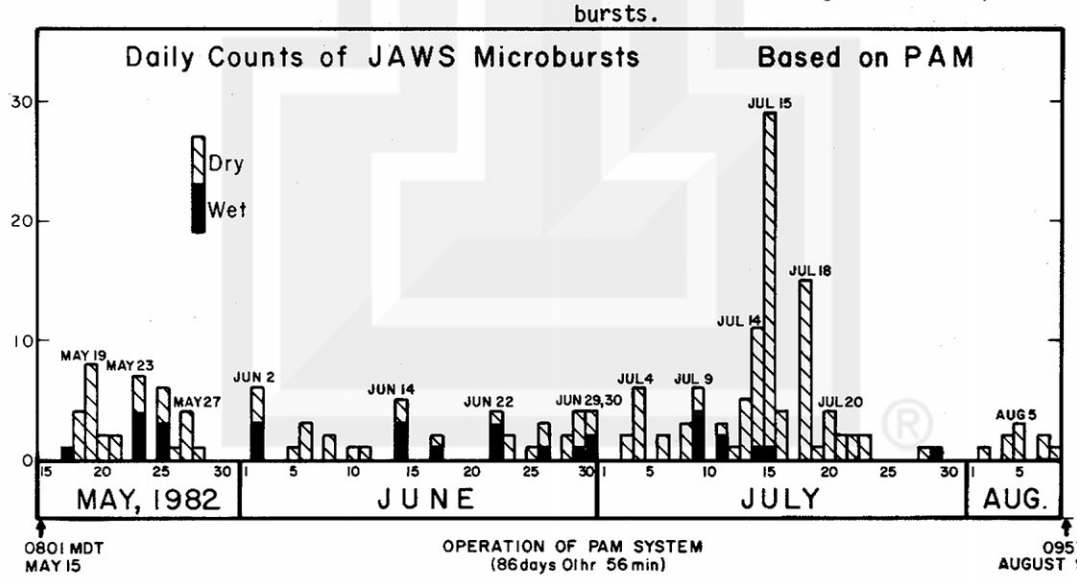

Fig. 6. Daily count of JAWS microbursts as determined by computer analysis. The number of wet and dry microbursts is shown on the figure.

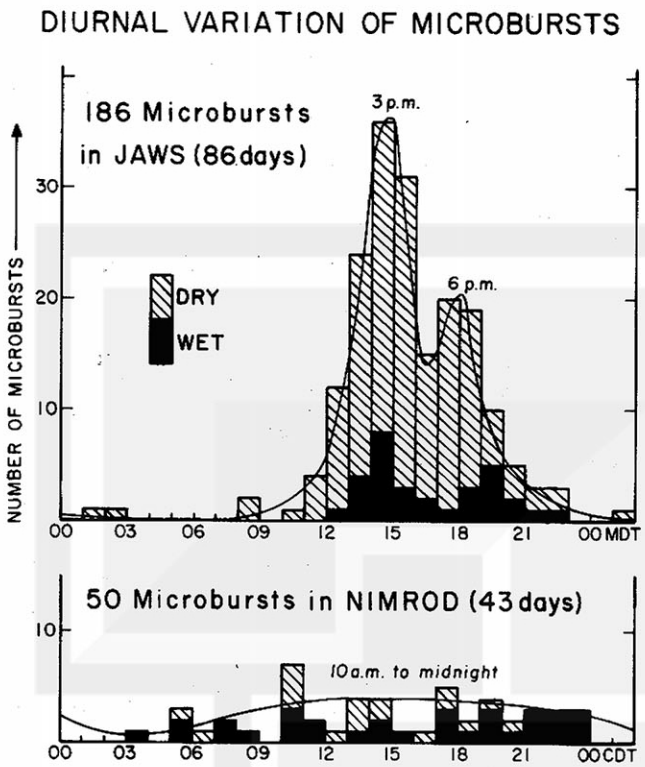

Fig. 7. Diurnal variation of surface microbursts. Top: 186 microbursts depicted during 86 days of JAWS operation. Two peak activity periods are 1500 and 1800 MDT. Bottom: 50 microbursts during 43 days of NIMROD operation. Rather uniform activity is seen from 1000 MDT to midnight.

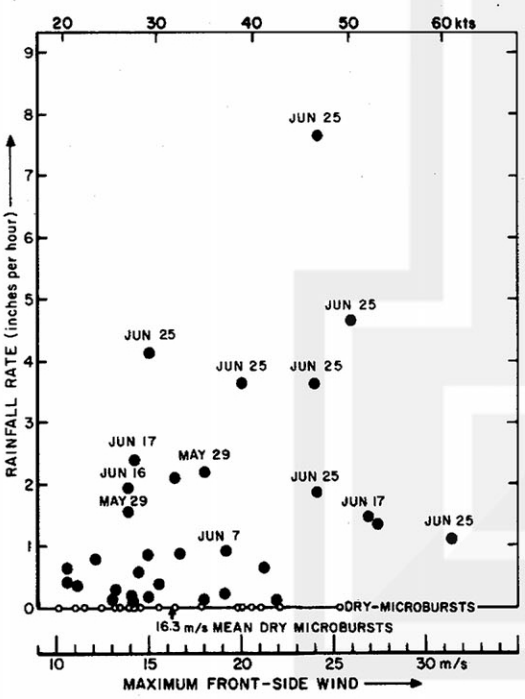

Fig. 8. Scatter diagram of the relationship between rainfall rate and the maximum wind speed of 50 microbursts during NIMROD.

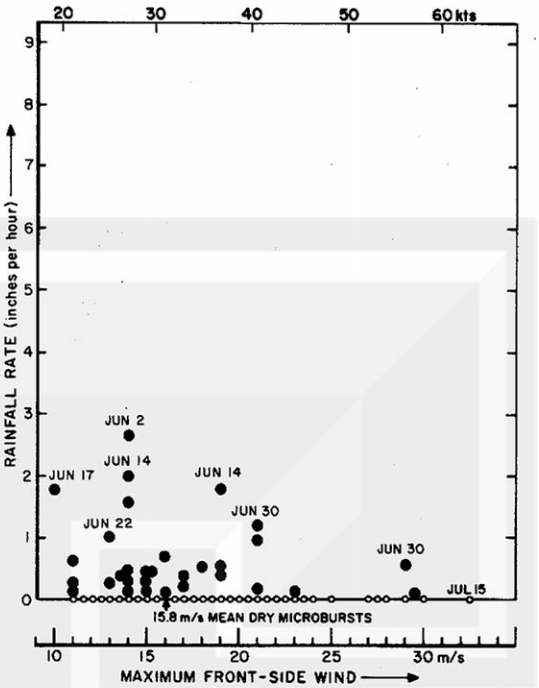

Fig. 9. Scatter diagram of the relationship between rainfall rate and the maximum wind speed of 186 microbursts during JAWS.

A similar analysis for the JAWS microbursts in Fig. 9 agree that outburst winds are practically independent of the rainfall rate. The highest microburst wind during the entire JAWS period, 36.6 m/s was induced by a dry microburst on July 15.

3.4 The Front-Side Maximum Winds

The highest wind in a translating microburst occurs on the frontside or the progressive side, where the outburst winds and the translational motion are toward the same direction. On the backside of a microburst, the resultant wind may blow toward the backside or the frontside, depending upon the relative strength of the outburst flow and the forward motion of the storm.

The frequency of the front-side maximum winds is shown in Fig. 10. The highest number of microbursts for JAWS and NIMROD are 13 m/s and 14 m/s, respectively, with both decreasing exponentially at higher wind speeds.

3.5 Front-to-Back or Total Wind Shear

Although the highest wind speeds occur on the front side of a translating microburst, the total wind shear, defined as the vector sum of the frontside to back-side wind is the most important variable for an aircraft penetrating through the center of a microburst. This velocity differential and its effect on aircraft performance has been discussed by Fujita & Caracena (1977) and Fujita (1983).

The front-to-back wind shear of the JAWS microbursts estimated by the PAM winds, was as high as 49 m/s which is believed to be unpenetrable to

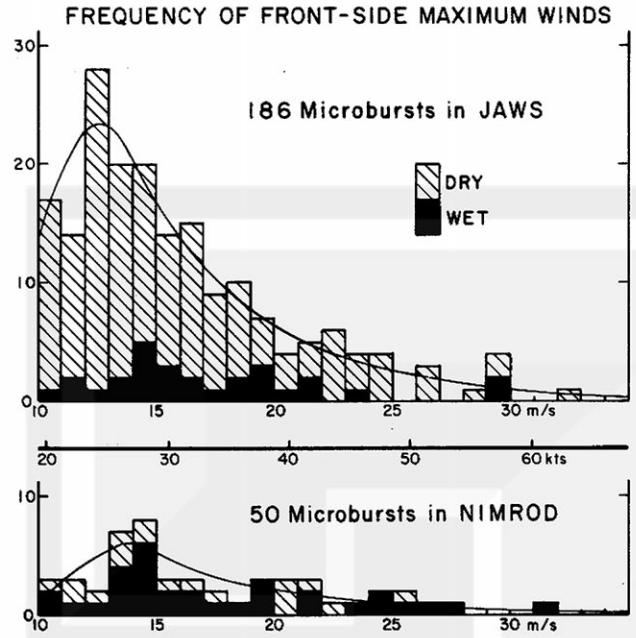

Fig. 10. Frequency of front-side maximum winds. The highest wind speeds in a translating microburst occurs on the front side where the outburst winds are superimposed upon the translational motion.

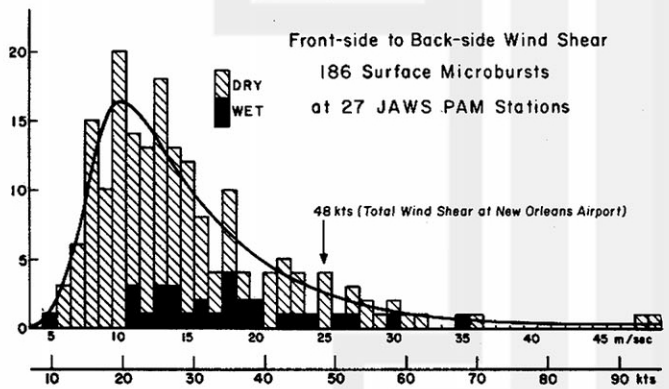

Fig. 11. Frequency of surface microbursts presented as a function of the front-side to back-side wind shear. An aircraft penetrating through a microburst from the front or the backside would experience this magnitude of wind shear.

an aircraft (see Fig. 11). The frequency in Fig. 11 peaks at 10 m/s and decreases exponentially at higher wind shear values. Table 1 depicts the cumulative frequency of JAWS microbursts in each of the front-side to back-side wind shear categories. The 48 kts (24.7 m/s) total wind shear of the New Orleans microburst ranks in the top 10% of the JAWS microbursts.

4. PARENT CLOUDS OF MICROBURSTS

The parent cloud of a microburst has been an important question to the authors during the past two field experiments. The conclusion after NIMROD was that the parent cloud was the cumulonimbus. However, during JAWS it became apparent that two additional types of clouds existed. These three types of parent clouds are summarized below:

Cumulonimbus - Wet and dry microbursts may descend from the dark base of a cumulonimbus, often accompanied by lightning and hail nearby. The intensity of the outburst winds is unrelated to that of the rainfall. In some instances, several thunderstorms organize into a bow-shaped echo on radar (Fujita, 1981; Forbes & Wakimoto, 1983; Wakimoto, 1983) which indicates possible downburst winds.

Spreading Anvil - Dry microbursts may develop beneath the long precipitation streaks falling from a spreading anvil of a dissipating cumulonimbus. Owing to the evaporation during the long descent, practically all of the microbursts are dry but the outburst winds may be very strong. Cloud-base detrainment instability as discussed by Emanuel (1981) may be applicable to this type of wind shear.

Cumulus Congestus - Streaks of virga descending from a cumulus congestus in its post-mature stage may appear innocuous, however, the virga could induce a strong microburst lasting 2 to 3 minutes. Most microbursts are dry. After the end of the microburst, the parent cloud loses its hydrometeors, often leaving a depression atop the cloud.

Table 1

Cumulative frequency of JAWS microbursts.

Wind shear (m/s)	5	10	15	20	25	30	35	40	45	50
number of microbursts	186	151	73	35	19	8	4	2	2	0
percentage	100	81	39	19	10	4	2	1	1	0

As previously mentioned, in spite of the different types of microbursts, one characteristic they have in common is the lack of correlation between the strength of the outburst winds and their rainfall rates. Therefore it is not surprising that the radar reflectivity of microburst-induced showers and virga is not related to the outburst wind speed. It was common to see innocuous showers associated with less than 35 dBZ radar echoes producing strong, dry microbursts. Apparently precipitation-loading is not essential to microburst formation.

5. THE DRY MACROBURST AND MICROBURST OF 14 JULY 1982

The third most active wind shear day during JAWS was July 14, when almost all of the microbursts were dry. A microburst landed east of Denver ∿1430 MDT and subsequently expanded in all directions. By 1436 MDT the surface outflow had become a macroburst, as determined from aerial photography of dust clouds and surface PAM data (Fig. 12). Dual-Doppler wind vectors at a height of 200 m AGL are shown in Fig. 13. The largest velocities are toward the east; the same direction as the parent cloud motion. The maximum surface speed was 27 m/s which is comparable to the speeds at 200 m. Fig. 14 depicts dual-Doppler wind vectors at 820 m AGL combined with the wind measurements by the Wyoming King Air. The maximum reflectivity values at this level were slightly larger than 30 dBZ.

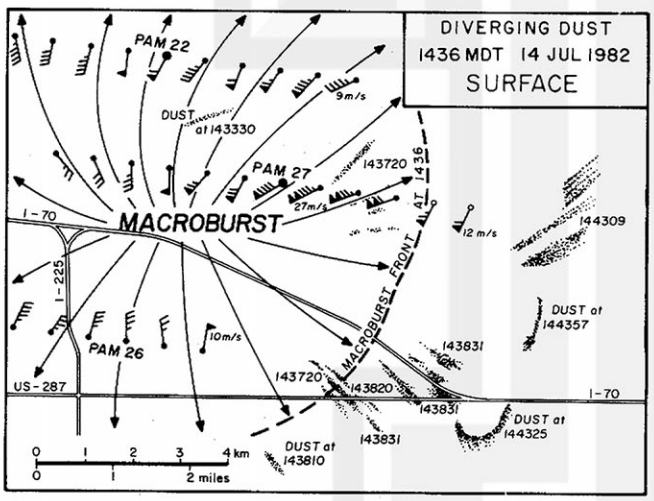

Fig. 12. Surface wind field of a macroburst at 1436 MDT. The dust locations were determined from aerial photography.

At 1800 m AGL (Fig. 15), there is very little outflow above the surface macroburst suggesting that the strongest velocities are confined to less than 820 m. A curious feature in the figure is a misocyclone (sub-mesoscale) that is just west of the macroburst front at the surface. The reflectivity pattern is similar to a LEWP (Line Echo Wave Pattern) but the circulation is less than 4 km. The misocyclone is still evident in reflectivity pattern at 1441 MDT as shown in Fig. 16. This type of rotation was often observed before the formation of a microburst at the surface. Approximately 30 minutes after the analysis time in Figs. 12-15, a

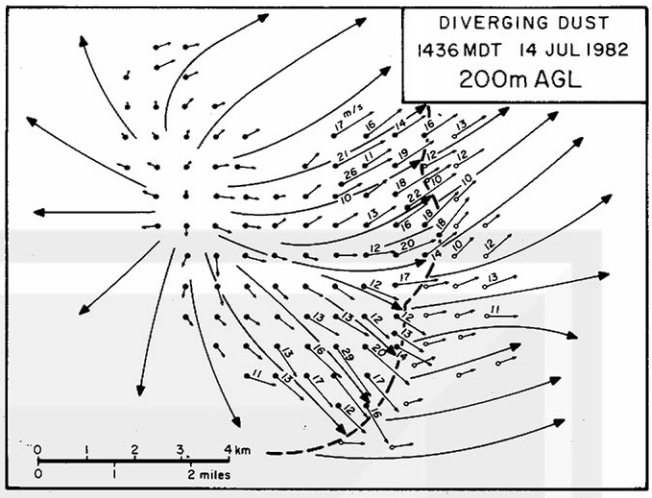

Fig. 13. Dual-Doppler wind field of a macroburst at 200 m AGL.

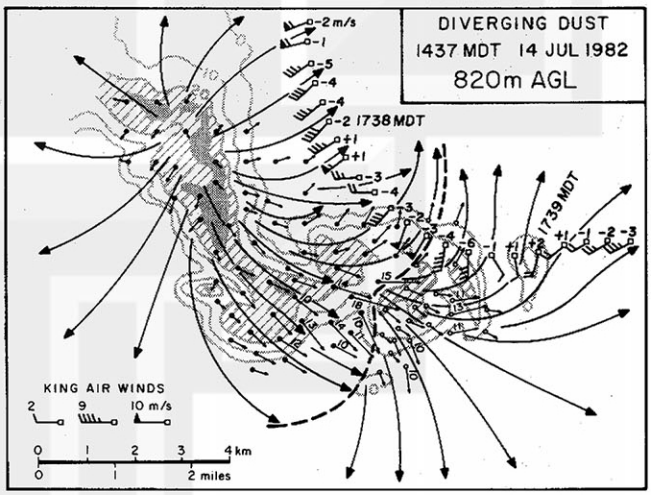

Fig. 14. Dual-Doppler wind field and the Wyoming King Air measurements of a macroburst at 820 m AGL. The gray areas denote radar reflectivities. The speeds labeled near the aircraft-derived wind vectors are vertical velocities.

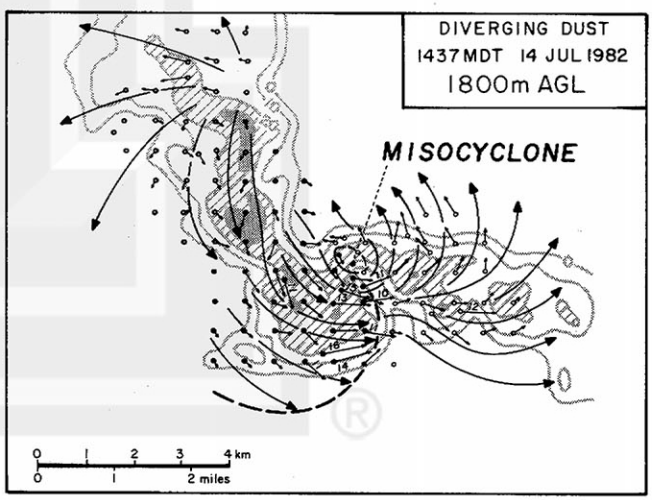

Fig. 15. Dual-Doppler wind field of a macroburst at 1800 m AGL. The gray areas denote radar reflectivities. A misocyclone is clearly indicated by the motion field.

strong microburst touched down from the same parent cloud resulting in tremendous amounts of dust being carried aloft into the lower boundary layer.

Data from this and other cases suggest that microburst winds are spawned from rotating downdrafts which originate from misocyclones such as one depicted in Figs. 15 and 16. Such precursors will be important for real-time warnings of wind shear events.

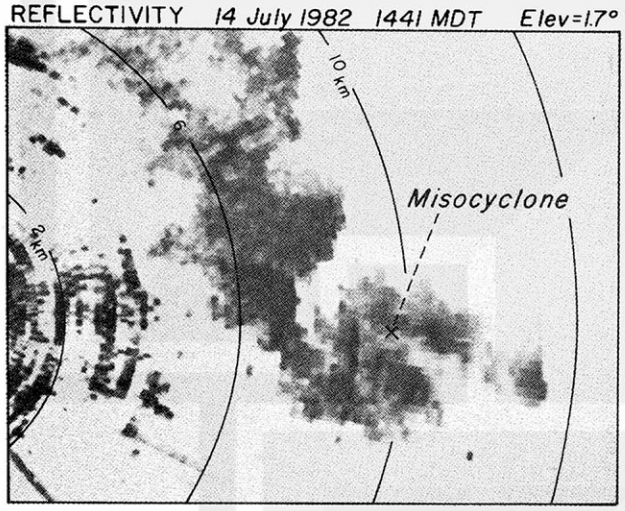

Fig. 16. Reflectivity pattern at 1441 MDT. Elevation angle is 1.7°. The misocyclone location is labeled on the figure.

6. CONCLUSIONS

The microburst is a relatively new finding in meteorology that has been shown in the past to have a significant effect on airline operations. It was believed that this phenomenon was spawned from intense thunderstorms, however, preliminary results from JAWS clearly indicate that the parent cloud may be a spreading anvil from a thunderstorm or a cumulus congestus cloud with radar reflectivities less than 35 dBZ. Visually the latter two cloud formations appear benign to an aircraft pilot. Moreover, the maximum wind speeds are not related to the rainfall rate which implies that an innocuous virga shaft may induce a dangerous wind shear event while an ominous-looking shower may be penetrable to an aircraft.

Dual-Doppler radar data has shown the existence of a misocyclone which precedes the formation of a surface microburst. The recognition of this signature in real time with a single Doppler radar will be important for protecting airports from the microburst hazard.

Statistics based on PAM data have shown that there are significant differences in microbursts depending on the geographic location. This suggests that the operation of a third project in a relatively wet area (i.e. southeastern U.S.) is required. After the conclusion of this proposed project, the results should be carefully related with those from the other two, to produce generalized results that can be applied nationwide.

Acknowledgements:

The authors wish to express their appreciation to all the scientists who were involved with the operation of the JAWS Project. Many of the PAM calculations were performed on the NCAR computers. This research has been sponsored by NSF under grant NSF/ATM 8109828, by NASA under grant NGR 14-001-008, and by NOAA under grant NA80AA-D-00001.

REFERENCES

Charba, J., 1974: Application of the gravity current model to analysis of squall-line gust fronts. Mon. Wea. Rev., 102, 140-156.

Emanuel, K., 1981: A similarity theory for unsaturated downdrafts within clouds. J. Atmos. Sci., 38, 1541-1557.

Forbes, G.S. and R.M. Wakimoto, 1983: A concentrated outbreak of tornadoes, downbursts, and microbursts, and implications regarding vortex classification. Mon. Wea. Rev., 111, 220-235.

Fujita, T.T., 1979: Objectives, operation, and results of Project NIMROD, Preprints, 11th Conf. on Severe Local Storms, Kansas City, Amer. Meteor. Soc., 259-266.

Fujita, T.T., 1980: Misoscale structure of downbursts depicted by Doppler radar. SMRP Res. Pap. No. 181, Dept. of the Geophysical Sci., Univ. of Chicago, 19 pp.

Fujita, T.T., 1981: Tornadoes and downbursts in the context of generalized planetary scales. J. Atmos. Sci., 38, 1511-1534.

Fujita, T.T., 1983: Microburst wind shear at New Orleans International Airport, Kenner, Louisiana on July 9, 1982., SMRP Res. Pap. No. 199, Dept. of the Geophysical Sci., Univ. of Chicago, 39 pp.

Fujita, T.T., and H.R. Byers, 1977: Spearhead echo and downburst in the crash of an airliner. Mon. Wea. Rev., 105, 129-146.

Fujita, T.T., and F. Caracena, 1977: An analysis of three weather-related aircraft accidents. Bull. Amer. Meteor. Soc., 58, 1164-1181.

Fujita, T.T. and R.M. Wakimoto, 1981: Five scales of airflow associated with a series of downbursts on 16 July 1980. Mon. Wea. Rev., 109, 1438-1456.

Fujita, T.T., and R.M. Wakimoto, 1982: Effects of miso- and mesoscale obstructions on PAM winds obtained during Project NIMROD. J. Appl. Meteor., 21, 840-858.

Goff, R.C., 1976: Vertical structure of thunderstorm outflows. Mon. Wea. Rev., 104, 1429-1440.

McCarthy, J., J.W. Wilson, and T.T. Fujita, 1982: The Joint Airport Weather Studies Project. Bull. Amer. Meteor. Soc., 63, 15-22.

National Transportation Safety Board, 1983: Aircraft accident report: Pan American World Airways, Inc., Clipper 759, Boeing 727-235, N4737, New Orleans International Airport, Kenner, Louisana, July 9, 1982. NTIS PB83-910402, 113 pp.

Wakimoto, R.M., 1982: The life cycle of thunderstorm gust fronts as viewed with Doppler radar and rawinsonde data. Mon. Wea. Rev., 110, 1060-1082.

Wakimoto, R.M., 1983: The West Bend, Wisconsin storm of 4 April 1981: A problem in operational meteorology. J. Clim. Appl. Meteor., 22, 181-189.